Dyes and Pigments 91 (2011) 120–125

Contents lists available at ScienceDirect

Dyes and Pigments

journal homepage: www.elsevier.com/locate/dyepig

Fabrication and properties of Acid Yellow 49 dye-intercalated layered double hydroxides film on an alumina-coated aluminum substrate

Pinggui Tang, Yongjun Feng, Dianqing Li*

State Key Laboratory of Chemical Resource Engineering, Beijing University of Chemical Technology, Box 98, 15 Beisanhuan Dong Lu, Beijing 100029, China

ARTICLE INFO

Article history:
Received 18 December 2010
Received in revised form
5 March 2011
Accepted 7 March 2011
Available online 16 March 2011

Keywords:
Film
Intercalation
Anion-exchange
Layered double hydroxides
Thermal stability
Light fastness

ABSTRACT

The Acid Yellow 49(4-[2-(5-amino-3-methyl-1-phenyl-1H-pyrazol-4-yl)diazenyl]-2,5-dichloro benzenesulfonic acid) (denoted as PPDB) anion intercalated layered double hydroxides (LDH) film was fabricated through an ion-exchange method using a ZnAl–NO_3–LDH/alumina/aluminum film as precursor. The prepared film was investigated by powder X-ray diffraction (XRD), Fourier transform infrared spectroscopy (FT-IR), Scanning electron microscopy (SEM), Thermogravimetric–differential thermal analysis (TG–DTA), UV–visible spectroscopy and the CIE 1976 L*a*b* color difference method. XRD patterns and FT-IR spectra confirm the successful incorporation of PPDB anions into the interlayer galleries of ZnAl–LDH with an expansion of d-spacing from 0.88 nm to 2.51 nm and the disappearance of characteristic absorption band of NO_3^- anions at 1384 cm^{-1}. The SEM morphologies show that the LDH films are mainly oriented with *c* axis of the platelet crystallites parallel to the substrate surface. Additionally, the obtained results suggest that the intercalation of PPDB into ZnAl–LDH host markedly improve the thermal stability and light fastness of PPDB.

1. Introduction

Layered double hydroxides (LDH), also known as hydrotalcite-like compounds, are a class of anionic layered clays with the general formula $[M^{2+}_{1-x}M^{3+}_{x}(OH)_2]^{x+}(A^{n-}_{x/n})\cdot mH_2O$ [$0.2 < x < 0.33$, typically abbreviated as $M^{2+}_{(1-x/x)}/M^{3+}-A-LDH$], where M^{2+} and M^{3+} individually stand for various di- and trivalent metal cations in the brucite-like host layers, and A^{n-} represents the interlayer guest anions in the hydrated interlayer galleries [1,2]. Based on their anion-exchange capability and compositional flexibility, LDH materials have received a great deal of attention due to their widespread applications as flame retardants [3], catalysts or catalyst precursors [4,5], adsorbents [6], anion-exchangers [7], drug delivery [8], polymer additives [9] and hybrid pigments [10,11].

Recently, LDH films have attracted considerable interest due to their novel properties and performances compared with their powdered forms, which will lead to an expansion in the applications of LDHs [12]. Usually, the LDH films are prepared by two methods: the physical deposition and the in situ growth or substrate-induced growth. In the former method, the substrate serves as a support for pre-synthesized LDH nanosheets or platelets. Two physical deposition methods are often used to fabricate such LDH films: the solvent evaporation method [13] and the layer-by-layer assembly method [14,15]; in the latter method, the substrate supplies the growing sites for the LDH film, and sometimes also acts as the source of metal cations needed for formation of LDHs. Substrates such as metal sheets [16,17], metal alloys [18,19], porous anodic alumina/aluminum [20], glass [21], sulfonated polystyrene [22], boehmite-coated materials [23] and Al_2O_3-coated materials [24] have been utilized to prepare LDH films by this method, which have the good mechanical strength and high adhesion to the substrate. The LDH films have been employed as heterogeneous catalysts [25], anti-corrosion coatings for metals [18], adsorbents [23], modified electrodes [26], components in optical or magnetic devices [27,28], and sensors [29]. However, there still remains a need for new functional LDH films.

Our previous studies have shown that the incorporation of some organic chromophore anions into the galleries of LDHs effectively enhances the thermal stability and light fastness [30,31]. Therefore colored functional films with excellent thermal stability and light fastness may be synthesized by intercalating dye anions into the interlayer galleries of films of LDHs. Such films can serve as paints which impart color and also provide protection for the substrate.

In this work, incorporation of Acid Yellow 49 (4-[2-(5-amino-3-methyl-1-phenyl-1H-pyrazol-4-yl)diazenyl]-2,5-dichlorobenzene sulfonic acid, abbreviated as PPDB) anions into a LDH film was

* Corresponding author. Tel.: +86 10 64436992; fax: +86 10 64425385.
E-mail address: lidq@mail.buct.edu.cn (D. Li).

0143-7208/$ – see front matter © 2011 Elsevier Ltd. All rights reserved.
doi:10.1016/j.dyepig.2011.03.012

carried out by an ion-exchange method using a ZnAl–NO_3–LDH film on alumina/aluminum substrate as a precursor, and the thermal stability and light fastness of the film were investigated. The PPDB is a bright yellow dye and widely used in textile dyeing, see its structural formula in Fig. 1. Although the thermal stability of the dye is quite good, its light fastness is poor which severely limits its range of applications. If the PPDB anions can be intercalated into the galleries of films of LDHs, its thermal stability and light fastness may be improved, allowing yellow coating films with excellent thermal stability and light fastness to be fabricated.

2. Experimental section

2.1. Materials

Ammonia ($NH_3 \cdot H_2O$), sodium hydroxide (NaOH), ammonium nitrate (NH_4NO_3), ethanol (C_2H_5OH) and zinc nitrate hexahydrate ($Zn(NO_3)_2 \cdot 6H_2O$) were A.R. grade reagents. Water was deionized and decarbonated, with an electrical conductivity less than 10^{-6} S cm^{-1}. The aluminum substrate (purity: >99.5%; thickness: 0.1 mm) was purchased from Shanghai Jingxi Chemical Technology Co. Acid Yellow 49 was a commercial product with a purity of 94% and recrystallized twice from water before use.

2.2. Preparation of ZnAl–NO_3–LDH/alumina/aluminum precursor film

The aluminum sheet was firstly treated with 0.5% NaOH solution in order to remove the oxidation on the surface according to the literature [16] and then further ultrasonically treated in water and ethanol for 10 min each. The preparation of the ZnAl–NO_3–LDH/alumina/aluminum precursor film was similar to that reported elsewhere [32]. Dilute ammonia (2.5%, 4.5 mL) was added to a solution of $Zn(NO_3)_2$ (0.025 M, 100 mL) and NH_4NO_3 (0.15 M) to make a milky white solution. The resulting solution was transferred to a conical flask and the Al substrate was immersed in the above solution. Then the flask was sealed and the reaction was carried out with magnetic stirring at 80 °C for 12 h. The resulting film was rinsed four times with water and then dried at 80 °C for 24 h.

2.3. Synthesis of ZnAl–PPDB–LDH/alumina/aluminum film

The PPDB anion intercalated film was prepared by the ion-exchange method using the ZnAl–NO_3–LDH/alumina/aluminum film as a precursor. The precursor film was immersed in the solution of PPDB (0.1 M, 100 mL) in a sealed beaker and maintained at 100 °C for 2.5 h. The film was then removed and rinsed five times with hot water and subsequently dried at 100 °C for 12 h.

2.4. Characterization

X-ray diffraction (XRD) patterns were obtained using a Shimadzu XRD–6000 diffractometer with monochromatic Cu K_α radiation ($\lambda = 0.15406$ nm) operating at 40 kV and 30 mA. FT-IR spectra were collected on a Bruker Vector 22 infrared spectrophotometer using the KBr disk method with a weight ratio of sample/KBr of 1:100. Thermogravimetric–differential thermal analysis (TG–DTA) curves were recorded on a PCT–IA instrument in the temperature range of 80–700 °C with a heating rate of 10 °C min^{-1} in flowing air. The morphology of the films was investigated by means of a scanning electron microscope (SEM, Hitachi S–3500N). The accelerating voltage applied was 20 kV. Elemental analyses for metal elements in the LDH powder scraped from film were performed using an ICPS–7500 model inductively coupled plasma emission spectrometer (ICP-ES). Carbon, hydrogen and nitrogen analyses were carried out on Elementar vario EL Analyzer. The color difference (ΔE) of materials aged under UV light was determined in terms of CIE 1976 L*a*b* using a TC-P2A automatic colorimeter. The CIE 1976 L*a*b* is a color scale based on the Opponent-Colors theory, among L*, a* and b* values indicate the level of light–dark, red–green and yellow–blue colors [33,34].

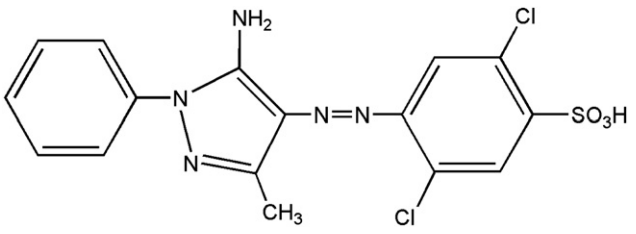

Fig. 1. The structural formula of Acid Yellow 49.

3. Results and discussion

3.1. Structure and morphology of the film

Elemental analysis results (wt%) of the powder scraped from the film: Zn = 43.13, Al = 10.61 for ZnAl–NO_3–LDH precursor; Zn = 21.79, Al = 4.79, C = 22.83, H = 3.26, N = 8.00 for ZnAl–PPDB–LDH. A little alumina in the powder scraped is detected as there is an alumina layer between the LDH crystallite and the aluminum substrate [16]. Based on Zn and C content, our evaluated results show that each molar ZnAl–PPDB–LDH with a formula of $Zn_{0.738}Al_{0.262}(OH)_2(PPDB^-)_{0.262} \cdot 0.71H_2O$ is mixed with ca. 0.064 M Al_2O_3 in the scraped powder.

Fig. 2 shows the XRD patterns of the aluminum substrate, ZnAl–NO_3–LDH film precursor, PPDB, ZnAl–PPDB–LDH film and ZnAl–PPDB–LDH powder scraped from the film. The XRD pattern of the ZnAl–NO_3–LDH film precursor displays both the characteristic peaks of the aluminum substrate and ZnAl–NO_3–LDH. The [003] and [006] reflections of the ZnAl–NO_3–LDH crystal phase appear at 10.06° and 20.18° (2θ), respectively. The basal d-spacing of the ZnAl–NO_3–LDH calculated from the Bragg equation is 0.88 nm, which agrees well with that reported in the literature [35].

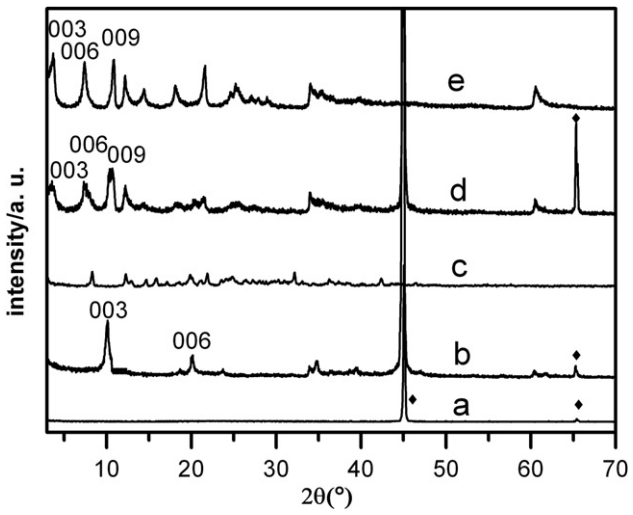

Fig. 2. XRD patterns of the aluminum substrate (a), ZnAl–NO_3–LDH film precursor (b), PPDB (c), ZnAl–PPDB–LDH film (d) and ZnAl–PPDB–LDH powder scraped from the film (e).

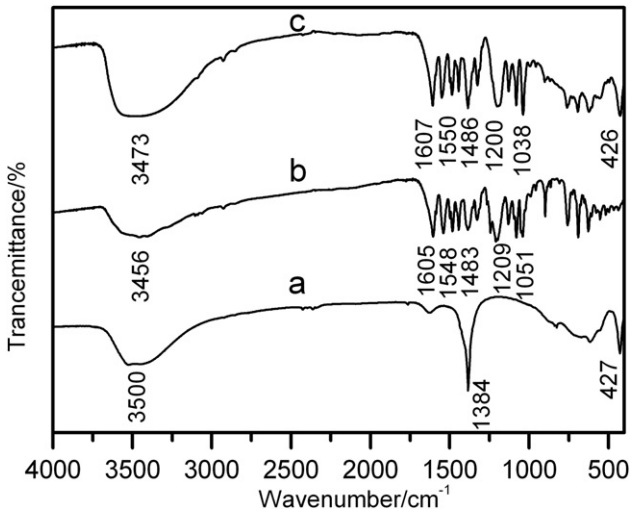

Fig. 3. FT-IR spectra of the powder scraped from the ZnAl–NO_3–LDH film precursor (a), PPDB (b) and ZnAl–PPDB–LDH powder scraped from the film (c).

Unlike the XRD pattern of powdered ZnAl–NO_3–LDHs which always show strong [00*l*] reflections, the [00*l*] reflections of the ZnAl–NO_3–LDH film precursor are relatively weak, which indicates that the LDH platelet crystallites mainly grew on the surface of aluminum with their *c* axis parallel to the substrate [28]. After reaction with PPDB, the diffraction peaks of the ZnAl–NO_3–LDH film precursor at 10.06° and 20.18° (2θ) disappears and two new diffraction peaks appears below 10°, suggesting that PPDB anions have been incorporated into the galleries of the ZnAl–LDH with an expansion of d-spacing from 0.88 nm to 2.51 nm because of the much larger size of PPDB than that of NO_3^- anion. This d-spacing of 2.51 nm is larger than the thickness of the brucite-like sheet (0.48 nm) plus the length of PPDB anion in the longest direction (ca. 1.68 nm), indicating that PPDB anions possibly arrange

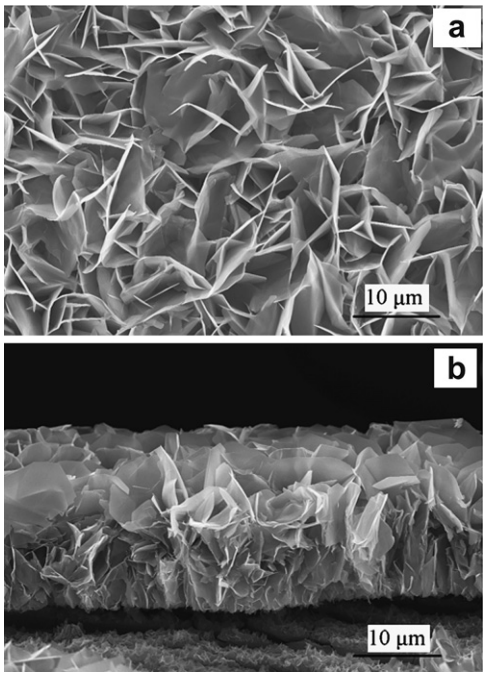

Fig. 4. SEM images of the top view (a) and cross-section view (b) of the ZnAl–NO_3–LDH film.

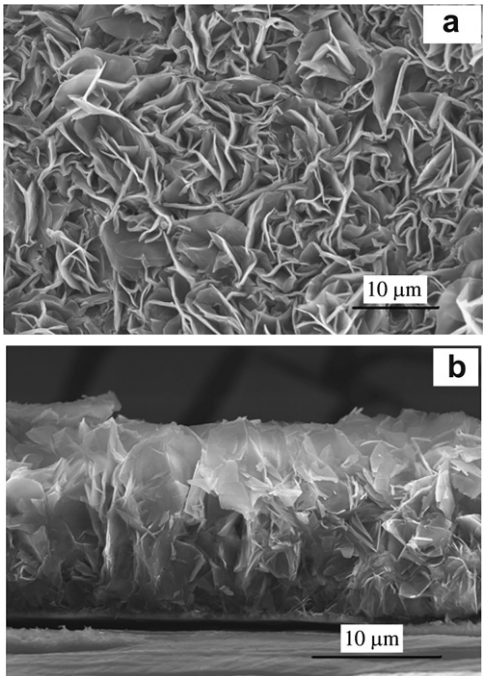

Fig. 5. SEM images of the top view (a) and cross-section view (b) of the ZnAl–PPDB–LDH film.

vertically to the LDH layers with an interdigitated structure in the interlayer region [36,37]. The XRD pattern of ZnAl–PPDB–LDH powder scraped from the film also shows sharp and symmetric [00*l*] reflection peaks as the precursor does, suggesting that the PPDB-intercalated LDH maintained a well-ordered layered structure.

Fig. 3 displays the FT-IR spectra of ZnAl–NO_3–LDH powder scraped from the film precursor, PPDB and ZnAl–PPDB–LDH powder scraped from the film. The spectrum of the ZnAl–NO_3–LDH powder scraped from the film precursor (Fig. 3a) has a broad absorption band centered at around 3500 cm^{-1}, which is assigned to the stretching vibrations of the hydroxyl groups of LDH layers and interlayer water molecules. The strong band at 1384 cm^{-1} is ascribed to the asymmetric stretching vibration of the intercalated nitrate anions and the absorption band at 427 cm^{-1} is attributed to the lattice vibrations of M–O–H [38]. The absorption bands at 1605, 1548 and 1483 cm^{-1} in the spectrum of PPDB correspond to the characteristic vibration bands of phenyl groups. The asymmetric and symmetric stretching vibrations of the $-SO_3^-$ group appear at 1209 and 1051 cm^{-1}, respectively.

The FT-IR spectrum of ZnAl–PPDB–LDH powder scraped from the film (Fig. 3c) shows the characteristic features of LDH materials together with the characteristic frequencies associated with the presence of PPDB anions. The broad band centered at around 3473 cm^{-1} is due to the OH stretching vibration of hydrogen-bonded interlayer water and hydroxyl groups on the layers and the characteristic absorption band of LDH materials at 426 cm^{-1} is attributed to the lattice vibrations of M–O–H. The absorption bands at 1607, 1550 and 1486 cm^{-1} are assigned to the vibration of phenyl groups of PPDB anions. The absorption bands of the asymmetric and symmetric stretching vibrations of the $-SO_3^-$ group appear at 1200 and 1038 cm^{-1} respectively. There are slight shifts in the positions of the absorption bands for asymmetric and symmetric stretching vibrations of the $-SO_3^-$ group, which can be ascribed to interactions between PPDB guest anions and the ZnAl–LDH host layers. Both of the XRD and the FT-IR results

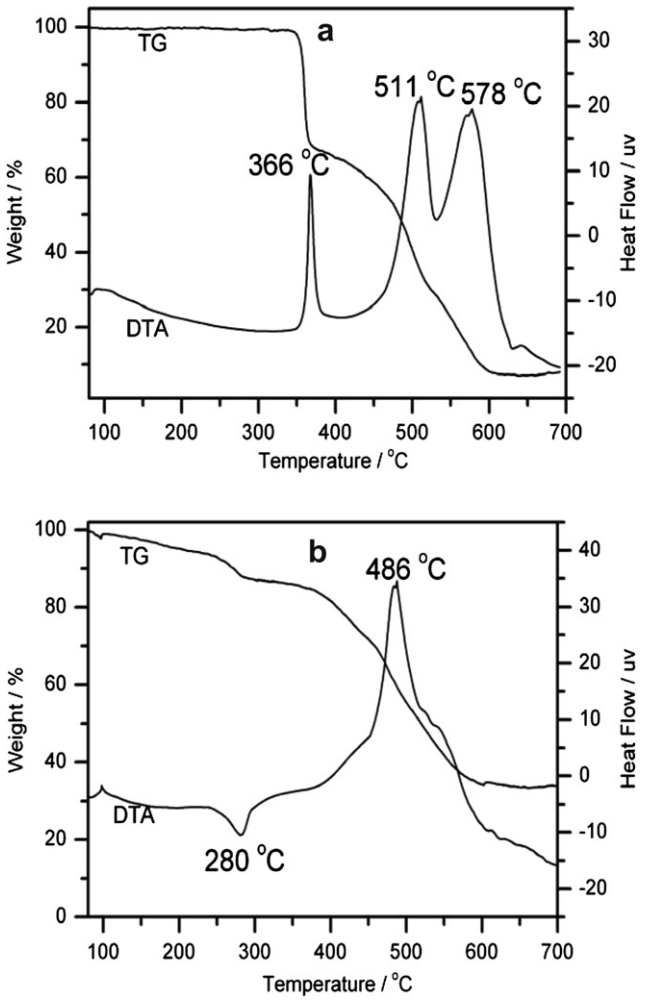

Fig. 6. TG–DTA curves of PPDB (a) and ZnAl–PPDB–LDH powder scraped from the film (b).

conclusively confirm the successful intercalation of PPDB anions into the galleries of ZnAl–LDH.

The morphology of the films was investigated by SEM and the images of the top view and cross-section view of the ZnAl–NO_3–LDH film precursor are depicted in Fig. 4. The ZnAl–NO_3–LDH film can be clearly observed with the LDH microcrystals covering the whole substrate with their curved hexagonal *ab* faces perpendicular to the substrate, similar to that reported in the literature [32]. The cross-section view (Fig. 4b) shows that the film consists of a continuous monolayer, constructed from hexagonal platelets grown vertically on the substrate, and has a thickness of about 15 μm. Fig. 5 depicts images of the top view and cross-section view of the ZnAl–PPDB–LDH film. Compared with the porous surface of the ZnAl–NO_3–LDH film precursor, the morphology of the ZnAl–PPDB–LDH film is somewhat different. The surface becomes much more compact and the LDH sheets turns to much thicker due to the expansion of the basal spacing after intercalation of PPDB anions. The cross-section view of ZnAl–PPDB–LDH film indicates that the thickness of film is about 16 μm, which is similar to that of the precursor film.

3.2. Thermal stability of the film

The TG–DTA curves of PPDB and ZnAl–PPDB–LDH powder scraped from the film are shown in Fig. 6. The TG curve of PPDB

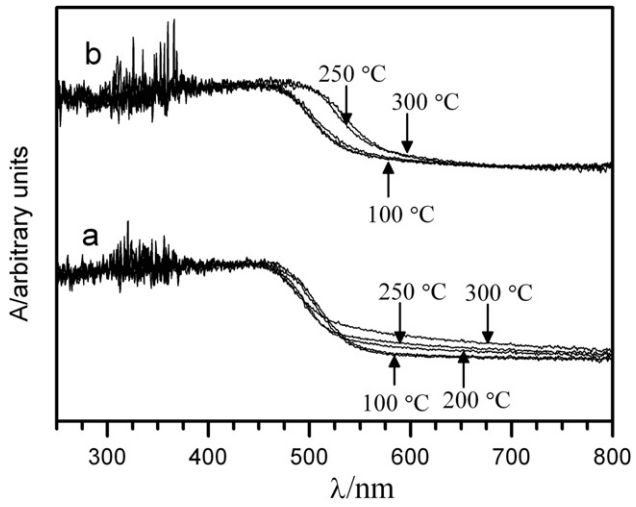

Fig. 7. UV–visible spectra of PPDB (a) and the ZnAl–PPDB–LDH film (b) after thermal aging at different temperatures.

displays two weight loss stages. The first weight loss stage from 80 to 400 °C, with a strong exothermic peak centered at 366 °C in the DTA curve, corresponds to the oxidative thermal decomposition of PPDB. The second weight loss stage from 400 to 700 °C is attributed to the combustion of the residue, and the DTA curve shows two strong exothermic peaks centered at 511 and 578 °C. The TG–DTA curve of ZnAl–PPDB–LDH powder scraped from the film is depicted in Fig. 6b. The TG curve also shows two mass loss stages. The first mass loss stage below 300 °C can be assigned to the loss of adsorbed water, and the removal of interlayer water as well as the dehydroxylation of the ZnAl–PPDB–LDH layers. Accordingly, the DTA curve displays an endothermic peak centered at around 280 °C corresponding to the dehydroxylation. The second mass loss stage from 375 to 700 °C is assigned to the oxidative thermal decomposition of the PPDB anions in the interlayer galleries of ZnAl–LDH with a broad exothermic peak centered at 486 °C in the DTA curve. Comparing the DTA curves of PPDB and ZnAl–PPDB–LDH, one sees that the temperature for oxidative thermal decomposition of PPDB anions in the interlayer galleries of ZnAl–PPDB–LDH is much higher than that for PPDB, which is possibly because of the interactions between the PPDB guest anions and the ZnAl–LDH host layers.

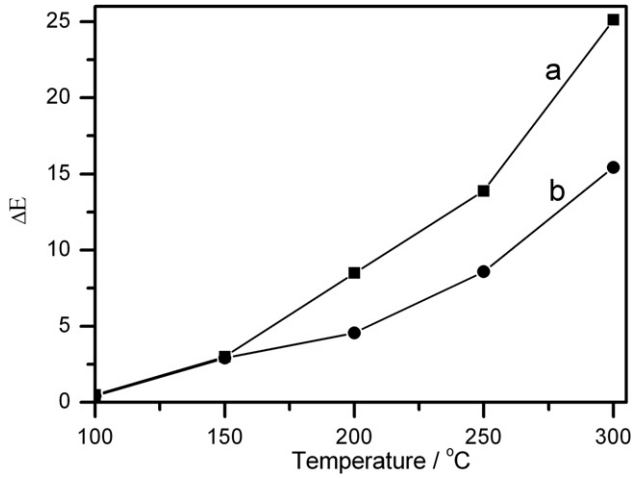

Fig. 8. Color difference (Δ*E*) values for PPDB (a) and the ZnAl–PPDB–LDH film (b) after thermal aging at different temperatures.

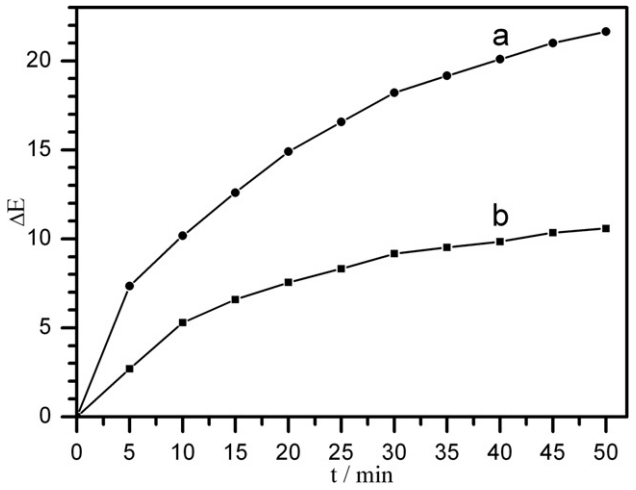

Fig. 9. Color difference (Δ*E*) values for PPDB (a) and the ZnAl–PPDB–LDH film (b) after UV aging for different times.

Fig. 7 demonstrates diffuse reflectance UV–visible spectra of the PPDB powder and the ZnAl–PPDB–LDH film which were heated in an oven at 100, 150, 200, 250, and 300 °C for 30 min, respectively. In Fig. 7 (a), the absorption spectrum in the range from 450 to 800 nm is significantly changed on heating at 200 °C. With increasing temperature, the changes in the spectrum become much more marked, indicating that the decomposition of PPDB begins at 200 °C. In the case of ZnAl–PPDB–LDH film, however, no change occurs in the spectrum after heated at 200 °C. The obvious change of the spectrum is observed in the range from 450 to 650 nm only after 250 °C, resulting from the dehydroxylation of the ZnAl–PPDB–LDH layers. These results mean that ZnAl–PPDB–LDH film can tolerate higher temperatures than PPDB. The color difference (Δ*E*) values (see Fig. 8) of the thermally aged samples were also measured using the CIE 1976 L*a*b* method. The Δ*E* values of PPDB are larger than those of ZnAl–PPDB–LDH film after thermal aging above 200 °C, confirming that the ZnAl–PPDB–LDH film has higher thermal stability than PPDB. Both of the above results suggest that the incorporation of PPDB anions into the interlayer galleries of ZnAl–LDH significantly improves the thermal stability of PPDB anions.

3.3. Light fastness of the film

Samples of PPDB and the ZnAl–PPDB–LDH film were photoaged in a UV photoaging instrument (with an ultraviolet high pressure mercury lamp as UV light source, 1000 W power and wavelength range 250–380 nm) equipped with a temperature control system. The color difference (Δ*E*) values of the irradiated samples (Fig. 9) were measured using the CIE 1976 L*a*b* method every 5 min up to a total exposure time of 50 min. The Δ*E* values for PPDB are considerably larger than those for ZnAl–PPDB–LDH after irradiation for the same time. The Δ*E* value of PPDB exceeds 21 after aging for 50 min, whereas the Δ*E* value for ZnAl–PPDB–LDH was less than 11. These results suggest that the light fastness of PPDB anions is enhanced by intercalation into the interlayer galleries of ZnAl–LDH.

4. Conclusions

A PPDB anion–pillared LDH film has been successfully prepared by an anion-exchange reaction using ZnAl–NO_3–LDH/alumina/aluminum film as the precursor in an aqueous solution of PPDB. The ZnAl–PPDB–LDH film constructed from hexagonal platelets perpendicular to the substrate covers the whole substrate and is compact. The intercalation of PPDB anions into the film of ZnAl–LDH has significantly enhanced the thermal stability and light fastness of PPDB anions. Therefore, this dye-intercalated ZnAl–LDH film has potentially practical applications. Furthermore, other color films with high thermal and photo stability can also be prepared by incorporating the corresponding organic chromophore anions into the galleries of LDHs.

Acknowledgments

This work was supported by National Natural Science Foundation of China (Grant No.: 20971013 and 21036001) and the 111 Project (Project No.: B07004).

References

[1] Cavani F, Trifirò F, Vaccari A. Hydrotalcite-type anionic clays: preparation, properties and applications. Catalysis Today 1991;11(2):173–301.
[2] Rives V, Angeles Ulibarri M. Layered double hydroxides (LDH) intercalated with metal coordination compounds and oxometalates. Coordination Chemistry Reviews 1999;181(1):61–120.
[3] Du B, Guo Z, Fang Z. Effects of organo-clay and sodium dodecyl sulfonate intercalated layered double hydroxide on thermal and flame behaviour of intumescent flame retarded polypropylene. Polymer Degradation and Stability 2009;94(11):1979–85.
[4] Halma M, Aparecida Dias de Freitas Castro K, Taviot-Gueho C, Prévot V, Forano C, Wypych F, et al. Synthesis, characterization, and catalytic activity of anionic iron(III) porphyrins intercalated into layered double hydroxides. Journal of Catalysis 2008;257(2):233–43.
[5] Kim MJ, Kim H, Jeong K-E, Jeong S-Y, Park YK, Jeon J-K. Catalytic decomposition of dibenzothiophene sulfones over layered double hydroxide catalysts. Journal of Industrial and Engineering Chemistry 2010;16(4):539–45.
[6] Pavlovic I, Pérez MR, Barriga C, Ulibarri MA. Adsorption of Cu^{2+}, Cd^{2+} and Pb^{2+} ions by layered double hydroxides intercalated with the chelating agents diethylenetriaminepentaacetate and meso-2,3-dimercaptosuccinate. Applied Clay Science 2009;43(1):125–9.
[7] Hu G-J, Wang H-X, Ling-Yan L, Pu M, He J, Evans DG. Supramolecular structural control and characteristics of p-hydroxybenzoate intercalated hydrotalcite. Journal of Physics and Chemistry of Solids 2010;71(9):1290–4.
[8] Tammaro L, Costantino U, Nocchetti M, Vittoria V. Incorporation of active nano-hybrids into poly([epsilon]-caprolactone) for local controlled release: antifibrinolytic drug. Applied Clay Science 2009;43(3–4):350–6.
[9] Qiu L, Chen W, Qu B. Morphology and thermal stabilization mechanism of LLDPE/MMT and LLDPE/LDH nanocomposites. Polymer 2006;47(3):922–30.
[10] Taviot-Gueho C, Illaik A, Vuillermoz C, Commereuc S, Verney V, Leroux F. LDH-dye hybrid material as coloured filler into polystyrene: structural characterization and rheological properties. Journal of Physics and Chemistry of Solids 2007;68(5–6):1140–6.
[11] Latterini L, Nocchetti M, Aloisi GG, Costantino U, Elisei F. Organized chromophores in layered inorganic matrices. Inorganica Chimica Acta 2007;360(3):728–40.
[12] Guo X, Zhang F, Evans DG, Duan X. Layered double hydroxide films: synthesis, properties and applications. Chemical Communications 2010;46(29):5197–210.
[13] Shi W, Wei M, Lu J, Li F, He J, Evans DG, et al. Molecular orientation and fluorescence studies on naphthalene acetate intercalated Zn_2Al layered double hydroxide. The Journal of Physical Chemistry C 2008;112(50):19886–95.
[14] Li L, Ma R, Ebina Y, Fukuda K, Takada K, Sasaki T. Layer-by-layer assembly and spontaneous flocculation of oppositely charged oxide and hydroxide nanosheets into inorganic sandwich layered materials. Journal of The American Chemical Society 2007;129(25):8000–7.
[15] Aradi T, Hornok V, Dékány I. Layered double hydroxides for ultrathin hybrid film preparation using layer-by-layer and spin coating methods. Colloids and Surfaces A: Physicochemical and Engineering Aspects 2008;319(1–3):116–21.
[16] Guo X, Xu S, Zhao L, Lu W, Zhang F, Evans DG, et al. One-step hydrothermal crystallization of a layered double hydroxide/alumina bilayer film on aluminum and its corrosion resistance properties. Langmuir 2009;25(17):9894–7.
[17] Zhang F, Zhao L, Chen H, Xu S, Evans D, Duan X. Corrosion resistance of superhydrophobic layered double hydroxide films on aluminum. Angewandte Chemie International Edition 2008;47(13):2466–9.
[18] Lin JK, Hsia CL, Uan JY. Characterization of Mg, Al-hydrotalcite conversion film on Mg alloy and Cl- and anion-exchangeability of the film in a corrosive environment. Scripta Materialia 2007;56(11):927–30.

[19] Wang J, Li D, Yu X, Jing X, Zhang M, Jiang Z. Hydrotalcite conversion coating on Mg alloy and its corrosion resistance. Journal of Alloys and Compounds 2010; 494(1–2):271–4.
[20] Chen H, Zhang F, Fu S, Duan X. In situ microstructure control of oriented layered double hydroxide monolayer films with curved hexagonal crystals as superhydrophobic materials. Advanced Materials 2006;18(23):3089–93.
[21] Guo X, Zhang F, Xu S, Evans D, Duan X. Preparation of layered double hydroxide films with different orientations on the opposite sides of a glass substrate by in situ hydrothermal crystallization. Chemical Communications 2009;(44):6836–8.
[22] Lei X, Yang L, Zhang F, Evans D, Duan X. Synthesis of oriented layered double hydroxide thin films on sulfonated polystyrene substrates. Chemistry Letters 2005;34(12):1610–1.
[23] Zhao Y, He S, Wei M. Hierarchical films of layered double hydroxides by using a sol-gel process and their high adaptability in water treatment. Chemical Communications 2010;46(17):3031–3.
[24] Zhao Y, Wei M, Lu J, Wang ZL, Duan X. Biotemplated hierarchical nanostructure of layered double hydroxides with improved photocatalysis performance. ACS Nano 2009;3(12):4009–16.
[25] Lü Z, Zhang F, Lei X, Yang L, Xu S, Duan X. In situ growth of layered double hydroxide films on anodic aluminum oxide/aluminum and its catalytic feature in aldol condensation of acetone. Chemical Engineering Science 2008;63(16):4055–62.
[26] Li M, Ni F, Wang Y, Xu S, Zhang D, Wang L. LDH modified electrode for sensitive and facile determination of iodate. Applied Clay Science 2009;46(4):396–400.
[27] Yan D, Lu J, Wei M, Evans DG, Duan X. Sulforhodamine B intercalated layered double hydroxide thin film with polarized photoluminescence. The Journal of Physical Chemistry B 2009;113(5):1381–8.
[28] Chen T, Xu S, Zhang F, Evans DG, Duan X. Formation of photo- and thermostable layered double hydroxide films with photo-responsive wettability by intercalation of functionalized azobenzenes. Chemical Engineering Science 2009;64(21):4350–7.
[29] Li X, Liu J, Ji X, Jiang J, Ding R, Hu Y, et al. Ni/Al layered double hydroxide nanosheet film grown directly on Ti substrate and its application for a nonenzymatic glucose sensor. Sensors and Actuators B: Chemical 2010;147(1):241–7.
[30] Guo S, Evans DG, Li D. Preparation of C.I. Pigment 52:1 anion-pillared layered double hydroxide and the thermo- and photostability of the resulting intercalated material. Journal of Physics and Chemistry of Solids 2006;67(5–6):1002–6.
[31] Tang P, Xu X, Lin Y, Li D. Enhancement of the thermo- and photostability of an anionic dye by Intercalation in a zinc–aluminum layered double hydroxide host. Industrial & Engineering Chemistry Research 2008;47(8):2478–83.
[32] Gao YF, Nagai M, Masuda Y, Sato F, Seo WS, Koumoto K. Surface precipitation of highly porous hydrotalcite-like film on Al from a Zinc aqueous solution. Langmuir 2006;22(8):3521–7.
[33] Senthilkumar M. Modelling of CIELAB values in vinyl sulphone dye application using feed-forward neural networks. Dyes and Pigments 2007;75(2): 356–61.
[34] Khan MAI, Ueno K, Horimoto S, Komai F, Someya T, Inoue K, et al. CIELAB color variables as indicators of compost stability. Waste Management 2009;29(12):2969–75.
[35] He H, Kang H, Ma S, Bai Y, Yang X. High adsorption selectivity of Zn–Al layered double hydroxides and the calcined materials toward phosphate. Journal of Colloid and Interface Science 2010;343(1):225–31.
[36] Liu L-Y, Pu M, Yang L, Li D-Q, Evans DG, He J. Experimental and theoretical study on the structure of acid orange 7-pillared layered double hydroxide. Materials Chemistry and Physics 2007;106(2–3):422–7.
[37] Costantino U, Coletti N, Nocchetti M, Aloisi GG, Elisei F. Anion exchange of methyl orange into Zn–Al synthetic hydrotalcite and photophysical characterization of the intercalates obtained. Langmuir 1999;15(13):4454–60.
[38] Kloprogge JT, Hickey L, Frost RL. FT-Raman and FT-IR spectroscopic study of synthetic Mg/Zn/Al-hydrotalcites. Journal of Raman Spectroscopy 2004;35(11): 967–74.